Applied Catalysis A: General 516 (2016) 70–80

Contents lists available at ScienceDirect

Applied Catalysis A: General

journal homepage: www.elsevier.com/locate/apcata

Preparation, kinetics, mechanism and properties of semi-transparent photocatalytic stable films active in dye degradation

Laura Suárez [a], César Pulgarin [a,*], Christophe Roussel [b], John Kiwi [a,**]

[a] Ecole Polytechnique Fédérale de Lausanne, EPFL-SB-ISIC-GPAO, Station 6, CH-101 Lausanne, Switzerland
[b] Ecole Polytechnique Fédérale de Lausanne, EPFL-SB-SCGC-GE, Station 6, CH-1015 Lausanne, Switzerland

ARTICLE INFO

Article history:
Received 31 October 2015
Received in revised form
30 December 2015
Accepted 28 January 2016
Available online 15 February 2016

Keywords:
PE-TiO_2
MB-discoloration kinetics
Photocatalyst stability
Reactive oxygen species
(ROS)-intermediates
Hydrophilic-hydrophobic balance
Redox Ti^{4+}/Ti^{3+}
XPS

ABSTRACT

The photocatalytic activity, mechanism and characterization of polyethylene-TiO_2 films (PE-TiO_2) during the discoloration/degradation of methylene blue (MB) are reported in this study. PE-TiO_2 films were prepared at moderate temperatures (~90 °C). TiO_2 did not leach out during discoloration/degradation of MB. This is a significant finding for a low temperature catalyst-polymer preparation leading to a stable repetitive MB degradation kinetics. MB discoloration on PE-TiO_2 films proceeded showing a quantum yield of 0.25%. Band-gap irradiation of TiO_2 was applied by way of a mercury medium pressure lamp to excite only TiO_2 and avoid MB photosensitization. The nature of the oxidative radicals intervening in MB discoloration was investigated by scavenging experiments. The relative importance of the oxidative species during MB discoloration is: $TiO_2 vbh^+ > HO_2^\bullet/O_2^{\bullet-} > {}^1O_2 > OH^\bullet$. Evidence is presented for the superoxide anion-radical $O_2^{\bullet-}$ at pH 6, as the main radical species leading to MB-discoloration. The MB- discoloration kinetic trend on PE-TiO_2 followed the behavior observed for diffusion-controlled reactions. The diffusion distance of the $HO_2^\bullet$ and $OH^\bullet$ radicals during the discoloration of a solution MB 1×10^{-5} mol L^{-1} were estimated as 71 and 2.2 μm respectively. The $OH^\bullet$ formation was assessed quantitatively during MB degradation by fluorescence measurements. The PE-TiO_2 film at time zero presented a contact angle (CA) of ~92°, decreasing within the five hour MB discoloration period to <5°. Reversibility from the hydrophilic nature of the film to the initial hydrophobic state proceeded in the dark within few days. The implications of the reversibility time on the MB-discoloration performance are discussed. Evidence for redox catalysis during MB-discoloration was found by XPS measurements. The surface properties of the (PE-TiO_2) films were characterized by X-ray fluorescence (XRF), UV–vis spectroscopy, X-ray photoelectron spectroscopy (XPS) and inductively coupled plasma mass-spectrometry (ICP-MS).

1. Introduction

The synthesis of environmentally friendly supported catalyst not needing high temperatures, organic solvents and expensive/sophisticated equipment is a primary focus of environmental catalysis/photocatalysis [1–6]. TiO_2 has been utilized for over four decades as the "golden standard" since it generates oxidative radicals under band-gap irradiation able to destroy pollutants and bacteria in the presence of air (O_2), (H_2O_v) and band gap photons [2,3]. Many studies have reported the photocatalyzed destruction of pollutants on TiO_2 coated surfaces like glass, iron plates and Raschig rings [5]. These are substrates with a high thermal resistance needing the annealing of TiO_2 up to few hundred degrees.

In the last decade many laboratories have focused on the discoloration degradation of pollutants/dyes on TiO_2 polymer films due to the polymers low-cost, high availability, stability, flexibility and corrosion resistance. Furthermore, PE films have UV-resistance, lack of oxidation in air, durability and chemical inertness. Polymer films have shown to be useful as catalyst supports leading to catalysis/photocatalysis with acceptable kinetics at the solid-air interfaces [6–11]. Some studies have reported a small absorption of organic compounds/dyes on PE in the dark.

TiO_2 nanoparticles have been attached on polymers from colloidal suspensions, dip coating, phosphonate coupling, chemical reduction, emulsion polymerization and spreading [14–20]. TiO_2 on polymers are generally coated by corroding the polymer

* Corresponding author.
** Corresponding author.
E-mail addresses: cesar.pulgarin@epfl.ch (C. Pulgarin), john.kiwi@epfl.ch (J. Kiwi).

http://dx.doi.org/10.1016/j.apcata.2016.01.041
0926-860X/

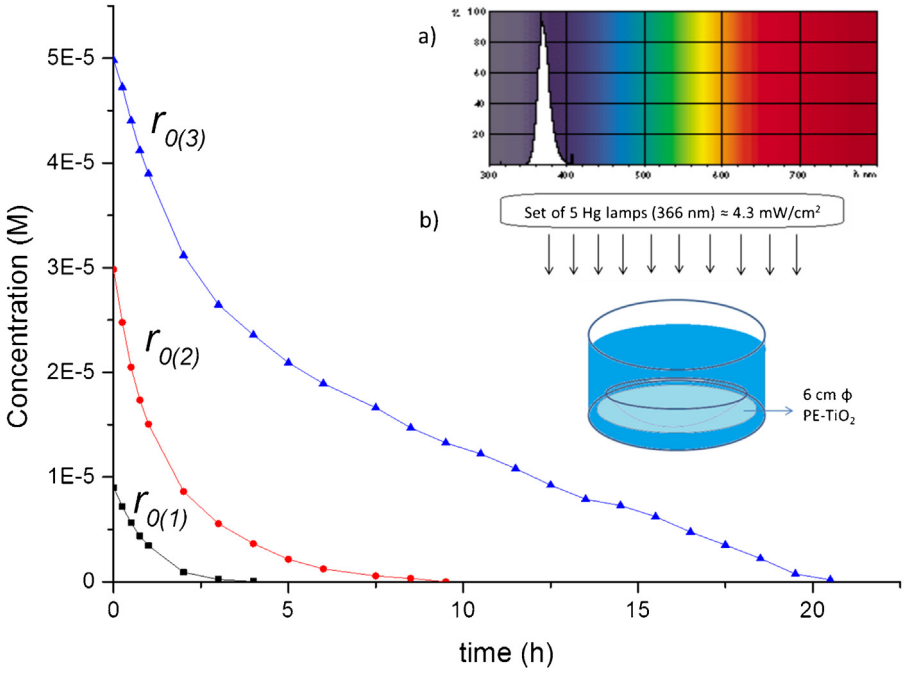

Fig. 1. Pseudo-first order rates of MB discoloration on PE-TiO_2 (0.90 TiO_2 wt%/wt PE) for different initial MB concentrations: 1) 1×10^{-5} mol L^{-1}, 2) 3×10^{-5} mol L^{-1}, 3) 5×10^{-5} mol L^{-1}. Inserts: a) Mercury lamps emission, 4.3 mW cm^{-2}, b) Reactor.

surface via organic solvents or TiO_2 under light. This induces on the substrate a sufficient number of TiO_2 binding sites [21–25]. More recently, PE-TiO_2 films have been prepared by sputtering techniques and shown to be successful in bacteria inactivation as well as in self-cleaning processes (MB) [26,27].

Methylene blue (MB) has been taken as the probe to test discoloration/degradation on PE-TiO_2. The photocatalytic properties of the PE-TiO_2 films were evaluated and the reactive oxygen species (ROS) unambiguously identified by selected scavenging experiments. TiO_2 supported films avoid the undesirable problem of TiO_2 recovery after the pollutant degradation in aqueous solutions. The latter process is expensive consuming time, labor and reagent costs.

The UV- and sunlight photo-activated MB degradation mediated by TiO_2 suspensions has been reported [1–6]. Under sunlight, both the MB and TiO_2 are photosensitized, MB injects electrons into the TiO_2cb and in parallel converts MB to the MB^{+*} cation radical [3,5]. Under visible light, the electron injected into the TiO_2 reacts with O_2 and generates highly oxidative radicals discoloring/degrading MB, shown below (1–5)

$$MB + \text{sunlight/visiblelight} \rightarrow MB* \quad (1)$$

$$MB + TiO_2 \rightarrow MB*^{+} + TiO_2\text{cbe-} \quad (2)$$

$$TiO_2\text{cbe-} + O_2 \rightarrow O_2^{\bullet -} \quad (3)$$

$$O_2^{\bullet -} + H^{+} \rightarrow HO_2^{\bullet} \quad (4)$$

$$MB*^{+} + HO_2^{\bullet} \rightarrow \text{mineralizationofMBproducts} \quad (5)$$

The present study on PE-TiO_2 films is warranted due to: the PE low-cost, corrosion resistance and high adhesion of TiO_2 on PE during repetitive MB-degradation. This study presents the low temperature deposition of TiO_2 on the PE polymer film (90 °C) leading to high adhesion of TiO_2 on PE. We have addressed only the UVA excitation of the PE-TiO_2. UV 366 nm light was applied to photoactivate specifically the TiO_2 avoiding the MB's photosensitization [28,29].

2. Experimental

2.1. Materials and PE-TiO_2 film preparation, MB discoloration kinetics, total organic carbon (TOC), X-ray fluorescence, irradiation sources, reactor geometry and actinometry

The low-density polyethylene (LDPE) is a highly branched low crystalline film with formula $H(CH_2\text{-}CH_2)_nH$. The (LDPE) 0.1 mm thick was obtained from Goodfellow, UK (ET311201). The film presented mechanical stability, had a density of 0.92 g cm^{-3} and was thermally stable up to 96 °C.

TiO_2 sols were prepared adding drop-wise a 1:1 volume mixture of Ti-isopropoxide and isopropanol to a 0.2 mol L^{-1} nitric acid solution and refluxing for 6 h. Then PE polymer films 6 cm diameter were cleaned with acetone and then coated with the TiO_2 sol. A second series of TiO_2 suspensions used dispersions of TiO_2 Degussa P25. The TiO_2 film deposition on PE was carried out by immersing the PE film in a TiO_2 30 g L^{-1} ethanol-suspension for 2 h under agitation. The films were then left to dry overnight, washed gently with de-ionized water and dried at 90 °C. Some other TiO_2 films were also prepared by using TiO_2 sol. The MB discoloration kinetics shown by the films prepared with TiO_2 sol were less reproducible compared to sol dispersions of TiO_2 Degussa P 25. For this reason, we focused on the last preparation throughout this study. The UV–vis spectra during MB discoloration were followed in an Schimadzu single beam instrument.

The total organic carbon (TOC) was determined in a Shimadzu TOC 500 equipped with an ASI auto-sampler. The Ti content in (PE-TiO_2) polymer films was evaluated by X-ray fluorescence in a PANalytical PW 2400 unit. A Philips low-pressure mercury vapor lamp model TL-D-15W/08 SLV was used for the photochemical experiments. The mercury lamp used provides an output of 1.2×1017 photons s^{-1} (4.3 mW cm^{-2}) at 366 nm.

The photochemical reactors used shown in the insert of Fig. 1 were cylindrical with a diameter of 8 cm and contained an MB volume set at 60 ml. Experiments were performed according to the ISO standards 10678: 2010 and 10676: 2010 [28] taking into consideration: a) initial pH of the MB-solution ~6, b) the use of BLB

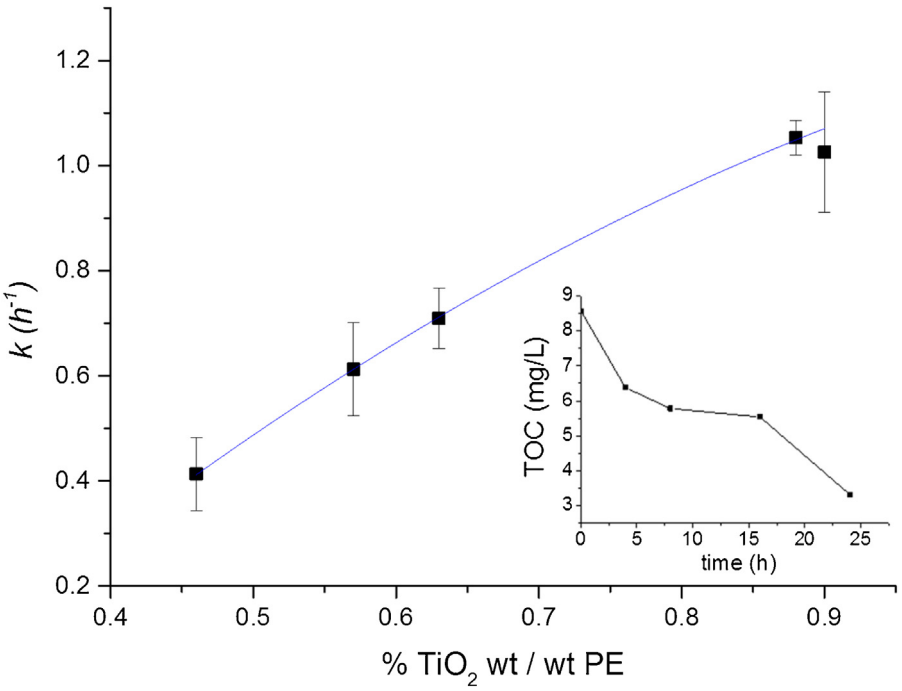

Fig. 2. Dependence of the pseudo-first order rate constant k, on the PE-TiO_2 loading, MB initial concentration: 1×10^{-5} mol L^{-1}. Insert. (a) Total organic carbon reduction for an aqueous solution MB 5×10^{-5} mol L^{-1} on a PE-TiO_2 film (0.90 TiO_2 wt%/wt PE). Mercury light irradiation 4.3 mW cm^{-2}.

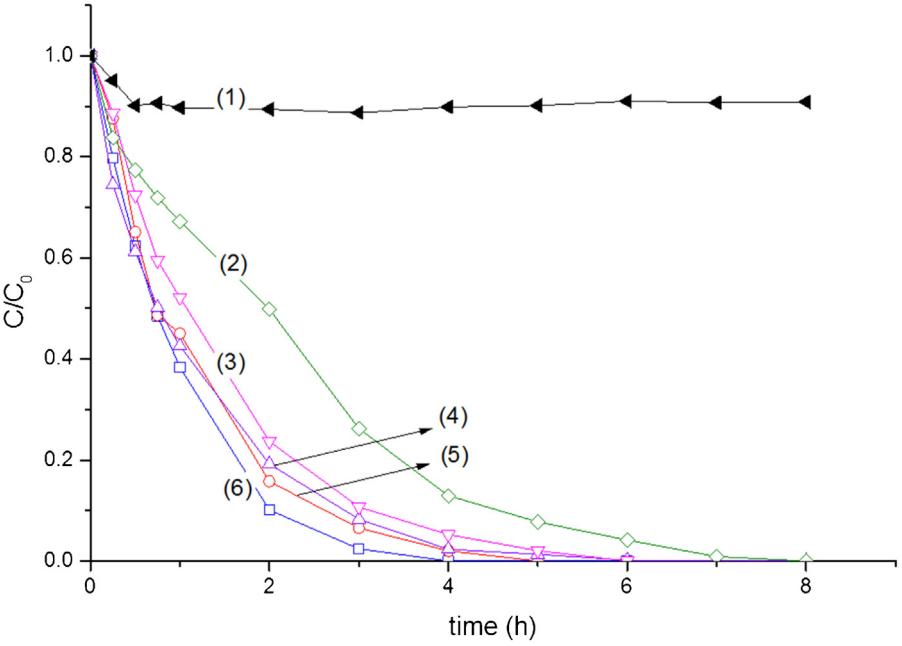

Fig. 3. MB 1×10^{-5} M discoloration as a function of time on (0.90 TiO_2 wt% PE-TiO_2) films at different mercury light intensities: (1) Dark run and runs underl ight on PE-TiO_2, (2) 1.1 mW cm^{-2}, (3) 1.9 mW cm^{-2}, (4) 2.8 mW cm^{-2}, (5) 3.5 mW cm^{-2}, (6) 4.3 mW cm^{-2}.

UVA light, c) stirring of the MB-solution during the reaction, d) the height of the solution in the reactor kept above 2 cm, e) pre-run equilibration of the MB-solution in contact with PE-TiO_2.

The actinometry addressed the photolytic reduction of Fe^{3+} to Fe^{2+} [14] with a quantum of 1.26 reported for light at 366 nm. Ferrioxalate ($K_3Fe(C_2O_4)_3 \cdot 3H_2O$) solutions were irradiated with a mercury light (366 nm) during different periods to obtain different concentrations of Fe^{2+}. The irradiated solutions were mixed with 1,10 phenanthroline 0.1% and buffered with $CH_3COONa \cdot 3H_2O$. This allowed the complexing reaction between Fe^{2+} and 1,10 phenanthroline. Subsequently, the Fe^{2+} was quantified by measuring the absorbance of the colored complex at 510 nm. The procedure described renders the amount of ferrous iron produced per unit of time (moles $Fe^{2+} s^{-1}$).

2.2. Intermediate ROS scavenging, determination of OH• by fluorescence and ICP-MS determination of Ti-ions leached out during MB discoloration

NaN_3 Fluka was used as oxygen singlet scavenger ($^1O_2$). 1,4-benzoquinone (BQ) and methanol were used respectively as $O_2^{\bullet -}$ radical scavenger and OH• scavengers [12]. Ethylenediamine tetra-

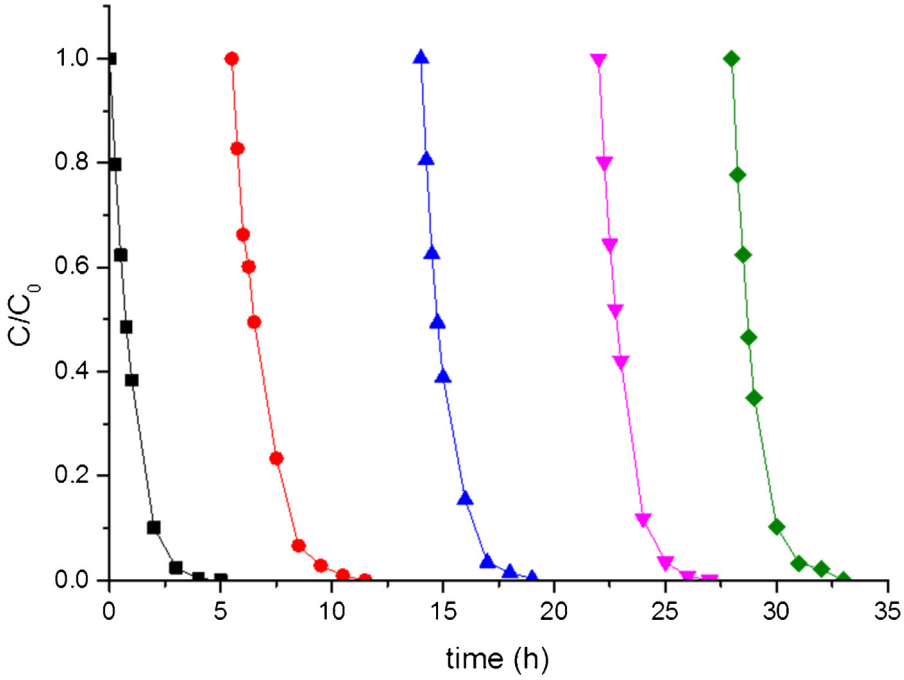

Fig. 4. Repetitive MB 1×10^{-5} mol L^{-1} discoloration as function of re-use on PE-TiO_2 (0.90 TiO_2 wt%/wt PE) films, Mercury irradiation 4.3 mWcm^{-2}.

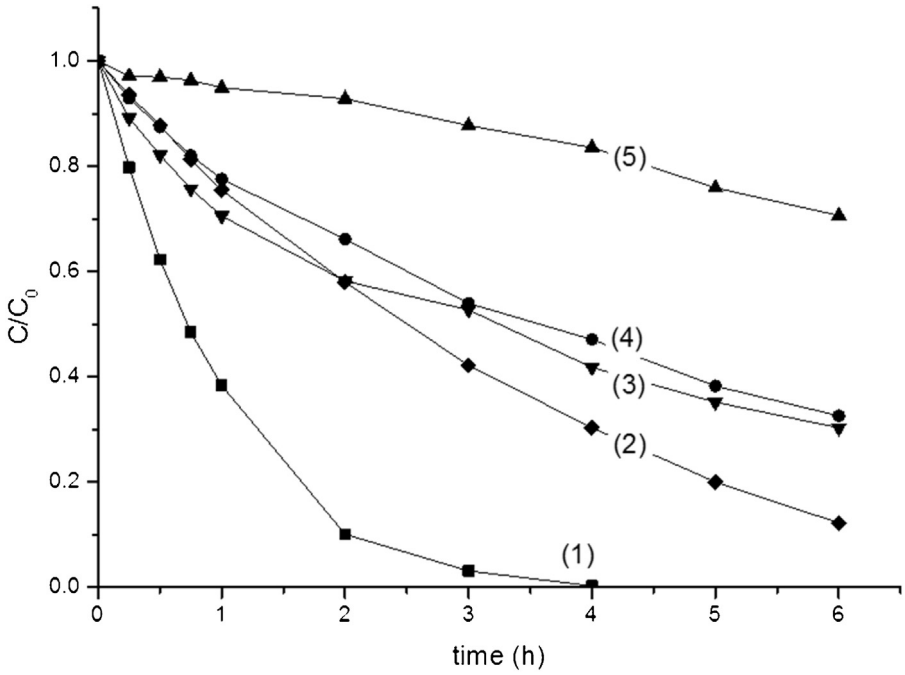

Fig. 5. MB discoloration on PE-TiO_2 of a solution MB 3×10^{-5} mol L^{-1}, PE-TiO_2: (0.90 TiO_2 wt%/wt PE) under mercury light 4.3 mW cm^{-2}. Scavengers used: Methanol 20 mmol L^{-1} ($HO^{\bullet}$), NaN_3 20 mmol L^{-1} ($^1O_2$), EDTA-2Na 20 mmol L^{-1} (h^+) and Benzoquinone(BQ) mmol L^{-1} ($O_2^{\bullet -}/HO_2^{\bullet}$): (1) No scavenger, (2) Methanol, (3) NaN_3, (4) BQ, (5) EDTA − 2Na.

acetic acid (EDTA-2Na) was used as TiO_2vb hole scavenger [13]. The quantification of the ROS (mainly $OH^{\bullet}$) was carried out based on the method proposed by Ishibashi et al. [30]. For this, 99% terephthalic acid from Across Chemical Ltd. as well as NaOH 98% from Sigma Aldrich were used. A round PE-TiO_2 sample of 6 cm diameter was immersed in a 0.4 mmol L^{-1} solution of terephthalic acid dissolved in a 4 mmol L^{-1} NaOH solution. After irradiation, the solution was transferred in a quartz cell. The fluorescence of the 2-hydroxyterephthalic-acid was quantitatively monitored on a Perkin Elmer LS-50B spectrometer. The spectra were recorded between 400 and 500 nm (scan rate: 100 nm/min) after excitation at 315 nm.

The determination by inductively coupled-plasma mass-spectrometry (ICP-MS) of the Ti eluted during MB degradation was carried out by a Finnigan™ ICP-MS unit equipped with a double focusing reverse geometry mass spectrometer. It has an extremely low background signal and a high ion-transmission coefficient. The PE-TiO_2 washing solution was digested with nitric acid 69% (1:1 $HNO_3 + H_2O$) to remove the organics in the solution and to guarantee that there were no remaining ions adhered to the flask wall. The

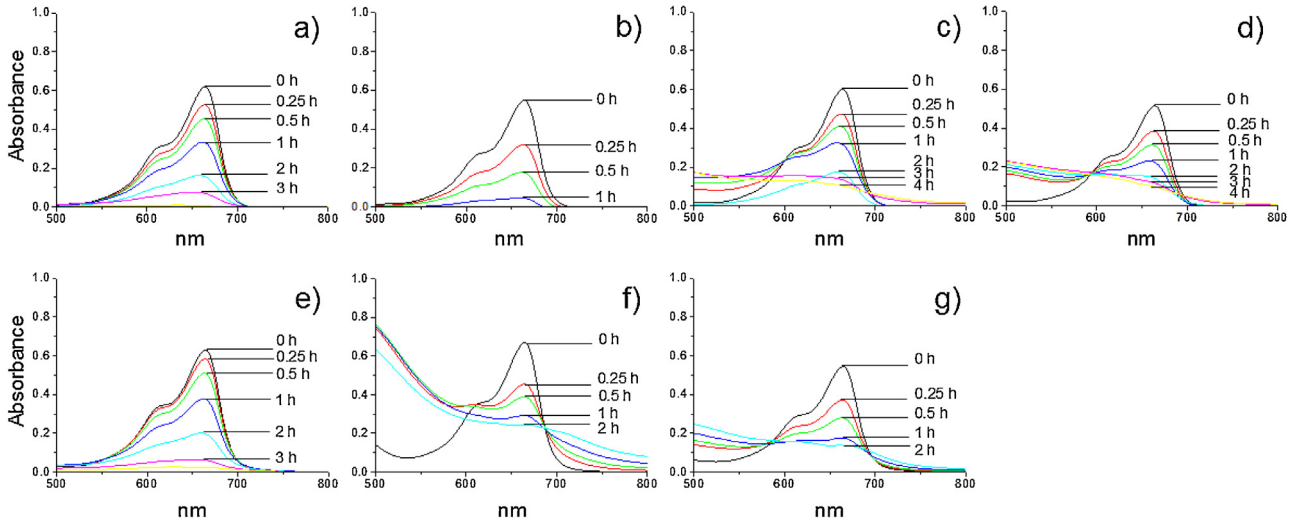

Fig. 6. MB 1×10^{-5} mol L^{-1}, discoloration on PE-TiO_2, PE-TiO_2 (0.9 TiO_2 wt%/wt PE); mercury lamps: 4.33 mW cm^{-2}: a) No scavenger at pH = 3, b) No scavenger at pH 6; c) BQ (2 mmol L^{-1}) at pH = 3, d) BQ (2 mmol L^{-1}) at pH = 6, e) NaN_3 (20 mmol L^{-1}) pH = 3; f) BQ (2 mmol L^{-1}) + NaN_3 (2 mmol L^{-1}) pH = 3; g) BQ (2 mmol L^{-1}) + NaN_3 (2 mmol L^{-1}) pH = 6.

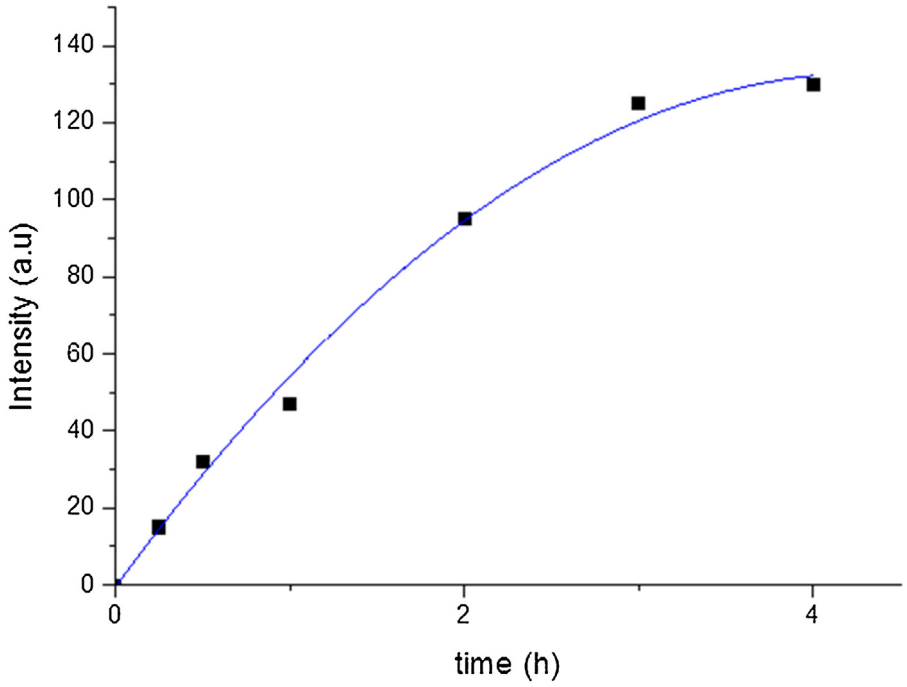

Fig. 7. Relative fluorescence increase in a solution 2-hydroxyterephthalic acid irradiated up to 4 h (mercury light 4.3 mW cm^{-2}) on a PE-TiO_2 (0.90 TiO_2 wt%/wt PE) sample.

samples droplets are introduced to the ICP-MS trough a peristaltic pump to the nebulizer chamber at ~7700 °C allowing the sample components evaporation and ionization. The Ti found in the nebulizer droplets was subsequently quantified by mass spectrometry (MS).

2.3. Absorption and contact angle determination (CA)

The optical density (OD) of the semitransparent PE-TiO_2 samples was measured in a Cary 16 spectrophotometer. Its absorbance measured in an aRTie F2-RT device since the samples presented some scattering. The hydrophilicity of the PE-TiO_2 films was determined on a Data Physics OCA 35 unit assessing the contact angle (CA) of a water droplet deposed by the sessile drop method.

2.4. X-ray photoelectron spectroscopy (XPS) of PE-TiO_2 films

An AXIS NOVA photoelectron spectrometer (Kratos Analytical, Manchester, UK) equipped with monochromatic AlK_α ($h\nu$ = 1486.6 eV) anode was used for this study. The XPS spectra were recorded by means of the software Casa XPS-Vision 2 (Kratos Analytical, UK).

3. Results and discussion

3.1. MB discoloration kinetics and effect of the TiO_2 loadings on the PE-TiO_2 films

Fig. 1 presents the initial discoloration rates (r_0) for MB on PE-TiO_2 (0.9 TiO_2 wt%/wt PE) films at different initial MB concen-

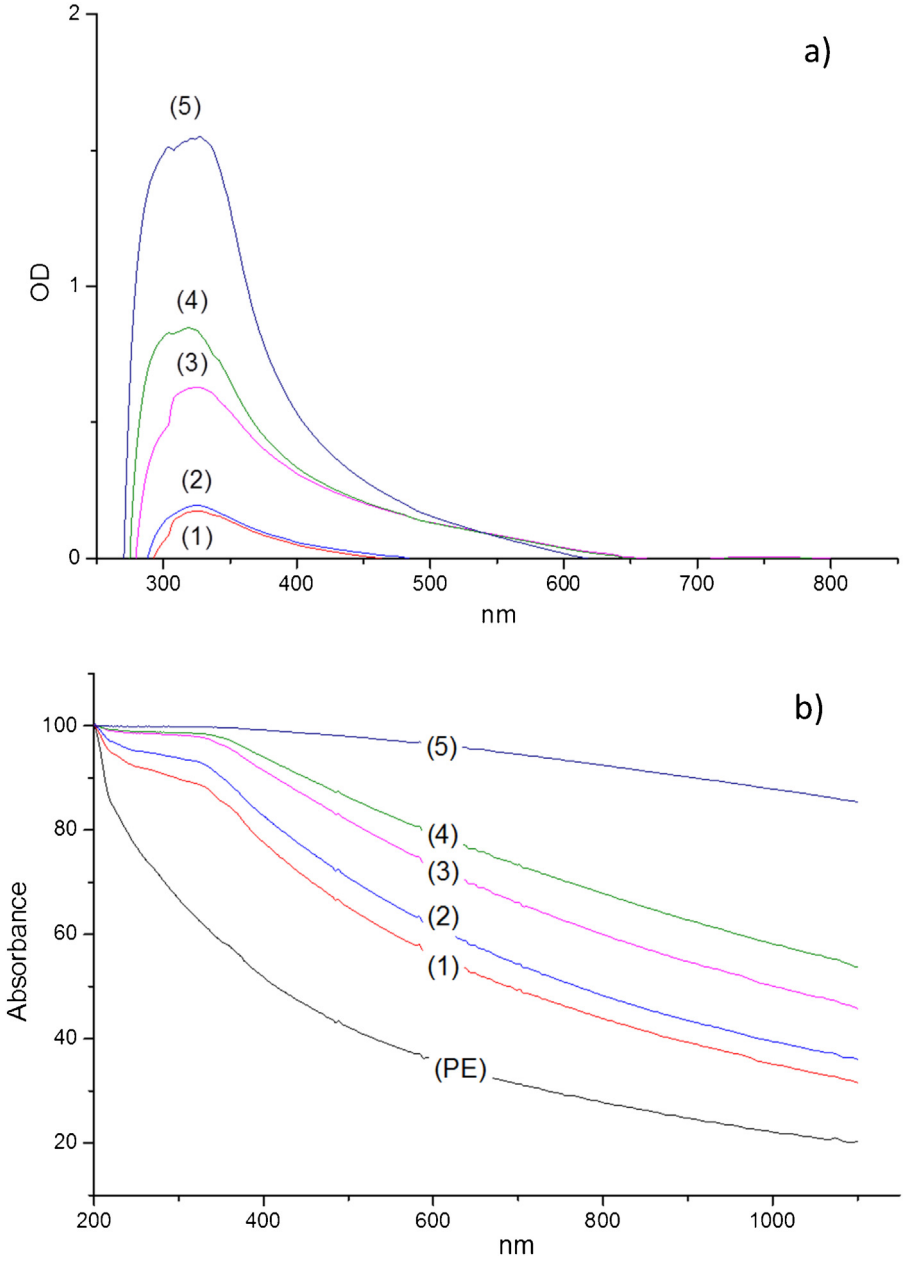

Fig. 8. a) Optical density (OD) of the PE-TiO_2 films: (1) 0.46 TiO_2 wt%/wt PE, (2) 0.57 TiO_2 wt%/wt PE, (3) 0.63 TiO_2 wt%/wt PE, (4) 0.88 TiO_2 wt%/wt PE, (5) 0.90 TiO_2 wt%/wt PE. b) absorbance of the PE films.

trations. These experimental runs were carried out following the ISO-standard for MB degradation described by A. Mills [5,28]. The MB-discoloration takes place due to the mercury light (366 nm) reaching the PE-TiO_2 surface, as MB presents an almost negligible optical absorption between 350 and 460 nm [3,6,26]. The evaluated concentrations are in the range of 10^{-5} mol L^{-1}. MB absorbance at 664 nm (strongest peak) was used to quantify the MB discoloration. For the runs under evaluation shown Fig. 1, the calculated initial discoloration rates were: $r_{0(1)}$ 7×10^{-6} mol L^{-1} h^{-1}, $r_{0(2)}$ 1.3×10^{-5} mol L^{-1} h^{-1} and $r_{0(3)}$ 1.1×10^{-5} mol L^{-1} h^{-1} for initial concentrations of 1×10^{-5} mol L^{-1}, 3×10^{-5} mol L^{-1} and 5×10^{-5} mol L^{-1} respectively. It is observed that as the initial concentration increases the initial discoloration rate increases as well. The proximity of the r_0 values corresponding to the two highest concentrations suggests that a nearly constant value of initial discoloration rate can be achieved for concentrations between 3×10^{-5} mol L^{-1} and 5×10^{-5} mol L^{-1}. The initial pH of the MB solution was pH 5.9–6.3 depending on the MB concentration in solution. Fig. 1 shows that MB discoloration proceeded from time zero. The electrostatic interaction between the cationic dye and the slightly positive TiO_2 (IEP ~ 6.6) seems to be low and not to hinder the contact of MB with the PE-TiO_2 film. Since the MB discoloration was determined by spectrophotometry, the rate constants reported in Fig. 1 not only refer to MB disappearance but might involve colored intermediates in solution. The overall quantum yield for MB degradation was ~0.25% as described in Section 2.1.

Fig. 2 shows the dependence of the rate constant k for the discoloration of MB on the TiO_2 loading of the PE films. A MB solution 1×10^{-5} mol L^{-1} was used for these experiments. Results show that the MB discoloration kinetics was proportional to the amount of

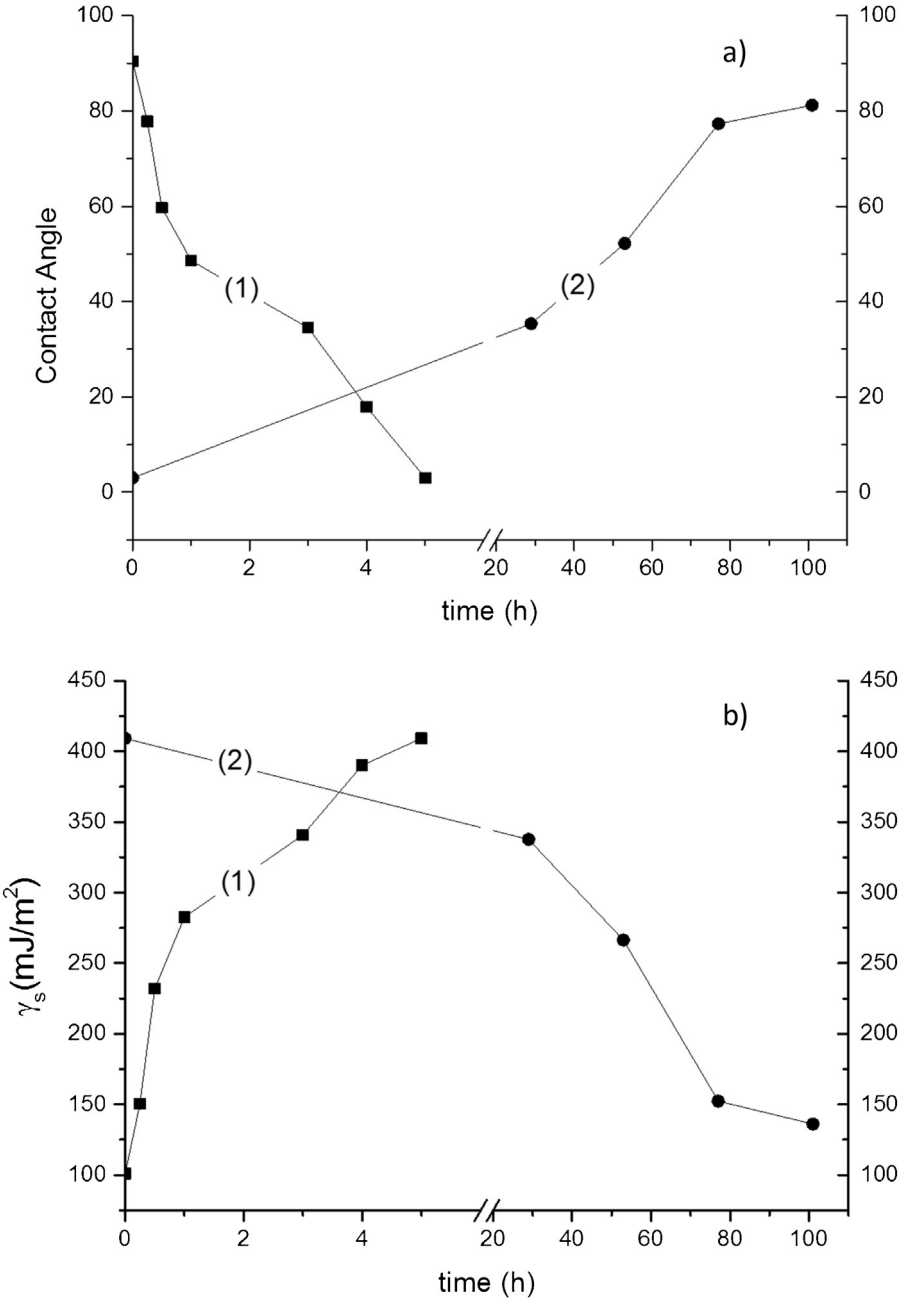

Fig. 9. Hydrophobic/hydrophilic transformations for a sample PE-TiO_2, (0.90 TiO_2 wt%/wt PE), under mercury light 4.3 mW cm^{-2} (1) hydrophobic to hydrophilic coversion under light, (2) hydrophilic to hydrophobic dark reverse reaction.

TiO_2 on the PE film, up to a TiO_2 content of 0.90 wt%/wt PE. A second order polynomial was used to fit the data presented and the correlation (R^2) found was 0.9963.

The insert in Fig. 2 shows a total organic carbon decrease (TOC) from 8.7 mg organic C L^{-1} to 3.5 mg organic C L^{-1} for a MB 5×10^{-5} mol L^{-1} solution. This concentration of MB was used for the TOC experiments because the reproducibility of the TOC data for a solution 5×10^{-5} mol L^{-1} was higher compared to a MB 1×10^{-5} mol L^{-1} solution. The elimination of all the TOC was not achieved. This agrees with the results reported by Houas et al. [31] reporting that long-lived C-containing intermediates were produced during the photocatalyzed degradation of MB on TiO_2 suspensions.

3.2. *Effect of light intensity on MB discoloration and ICP-MS evidence for the stable performance of PE-TiO_2 during repetitive use*

Fig. 3 shows the significant effect of the light intensity (photon flux) in the MB-discoloration kinetics. A small decrease of 5% was observed by MB absorption on PE-TiO_2 (Fig. 3, trace 1). MB adsorbs on the PE-TiO_2 film, which by itself does not degrade MB.

Table 1 presents mass ratio for the loading of TiO_2 on PE obtained by X-ray fluorescence (XRF) as a function of the TiO_2 Degussa P25 content of the suspension used during the preparation step. The quantum yield for the MB 1×10^{-5} mol L^{-1} discoloration under 5 lamps irradiation (4.3 mW cm^{-2}) was 0.25%. This latter value was

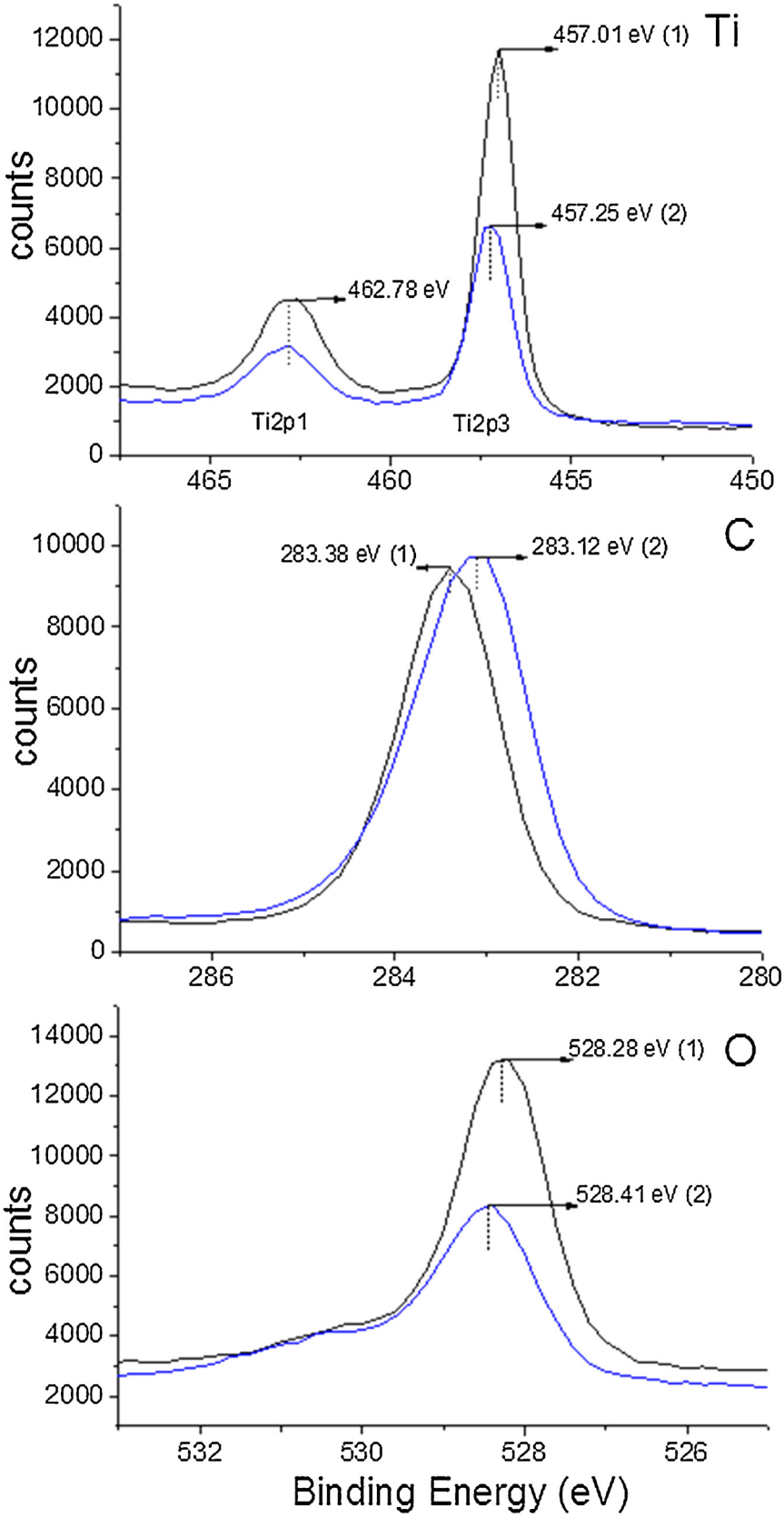

Fig. 10. XPS signals of Ti, C and O at: 1) time zero 2) after discoloration of a MB 3×10^{-5} mol L^{-1} solution, under mercury ligh irradiation 4.3 mW cm^{-2} on PE-TiO_2 films (0.90 TiO_2 wt%/wt PE).

Table 1
TiO_2 wt%/wt PE determined by X-ray fluorescence as a function of the TiO_2 content during the preparation of PE-TiO_2.

TiO_2 Degussa P25 suspension concentration (g/L)	TiO_2 wt%/wt PE	Experimental error (%)
2.5 g/L	0.46	0.02
5.0 g/L	0.57	0.02
10.0 g/L	0.63	0.02
20.0 g/L	0.88	0.03
30.0 g/L	0.90	0.03

estimated in the following way: a value Fe^{2+} of 1.26 was taken for the Fe $^{2+}$. The moles of photons s^{-1} were estimated (1.95×10^{-7} Einsteins s^{-1}). The transformed moles of MB per second were estimated as 4.93×10^{-10} mol s^{-1} from the degradation of a solution MB 1×10^{-5} mol L^{-1} on a sample PE-TiO_2: 0.9%TiO_2 wt/wt PE under a mercury light dose of 4.3 mW cm^{-2}. The amount of moles of MB per s^{-1} was then divided by the Einsteins s^{-1} to report the quantum efficiency of 0.25%.

In a separate set of experiments, degradation of MB at concentrations <10^{-5} were seen to require a lower number of photons to induce an acceptable MB-discoloration kinetics. Saturation effects were found in Fig. 3 during the irradiation of MB 1×10^{-5} mol L^{-1} when the number of photons was increased by a factor >4 by increasing the applied light intensity as shown in Fig. 3 traces 2 to 5. This shows that sufficient MB molecules were present to absorb higher levels of UVA photons cm^{-2} s^{-1}. Higher applied light intensities (traces (5,6) led to a slower increase in the MB-discoloration kinetics. A slower increase in the dye degradation kinetics was observed when the applied light intensity was increased during the degradation of colored pigments in commercial paints as reported by Egerton and King [32]. A change in the applied higher light doses in Fig. 3 affects less the MB-degradation compared to a variation of the light dose applied at low intensities.

The trend in the MB-discoloration times shown in Fig. 3 suggests that radical species generated at the PE-TiO_2 surface leads to MB-discoloration and the reactive oxygen species (ROS) diffuse within short distances. These distances can be estimated in the following way: a) a rate of production of $HO_2^\bullet$ ($k_a[HO_2^\bullet] \approx 10^6$ M^{-1} s^{-1}) has been reported for the reaction between the $HO_2^\bullet$ and anthracene, a molecule with a 3 ring structure close to MB [2,3]. For the reaction between $HO_2^\bullet$ and MB (1×10^{-5} mol L^{-1}), it is possible to assess the lifetime of the reaction-pair $HO_2^\bullet$ and MB as $\frac{1}{\tau} = k_a \left[OH_2^\bullet\right] [MB]$ with $k_aOH \approx 10^7$ M^{-1} s^{-1}. Next, we take in the Smoluchowski simplified relation $x^2 = D\tau$ a value of $D = 5 \times 10^{-6}$ cm^2 s^{-1} for the average value for low molecular weight molecules, in this case MB diffusing in aqueous solution. This leads to a value of 71 μm for the diffusion length of $HO_2^\bullet$, b) by a similar approach and taking for the $OH^\bullet$ $k_b[OH^\bullet] \approx 10^9$ M^{-1} s^{-1} leads to a diffusion length of ~2.2 μm for the $HO^\bullet$ away from the PE-TiO_2 films.

Fig. 4 shows the recycling use of a PE-TiO_2 sample up to the 5th cycle. No loss of activity was observed during the repetitive degradation of MB 1×10^{-5} mol L^{-1}. The sample was thoroughly washed after each recycling run. By ICP-MS, values <1 ppb Ti were detected as leaching out of the PE-TiO_2 sample after each recycling. This means that practically no TiO_2 could be detected out of the samples during repetitive MB-degradation. But when aMB sample 5×10^{-5} mol L^{-1} was discolored for 3 times, Ti concentrations between 14 and 28 ppb were detected. These latter concentrations of TiO_2 were not sufficient to degrade MB by themselves.

3.3. Scavenging of the oxidative species leading to MB degradation. Mechanism of reaction

Reactive oxygen species (ROS) are chemically reactive molecules containing oxygen, like superoxide, hydroxyl radical, and singlet oxygen. The different ROS radicals have been widely documented as being photo-induced by TiO_2 band-gap irradiation [4–6]. The contribution of these ROS in the study of MB degradation by PE-TiO_2 was monitored and is presented below in Fig. 5.

Fig. 5 presents the results of the scavenging of radicals in a MB 3×10^{-5} solution under band-gap irradiation up to 6 h. The relative contributions of the radicals generated at the PE-TiO_2 surface show: a) trace (1) MB discoloration mediated by PE-TiO_2, b) trace (2) MB discoloration in the presence of methanol 20 mmol L^{-1} a quencher of OH-radicals, c) trace (3) MB discoloration in the presence of NaN_3 20 mmol L^{-1} [2,3,35] a scavenger of oxygen singlet $^1O_2$, d) trace (4) MB discoloration in the presence of benzoquinone 20 mmol L^{-1} [33,34] a quencher of $O_2^{\bullet-}/HO_2^\bullet$ e) trace (5) MB discoloration in the presence of 20 mmol L^{-1} ethylene-diamine tetra-acetic acid disodium salt (EDTA-2Na), a widely used TiO_2vb(h^+) scavenger [1–3]. Based on the results shown in Fig. 5, the scavengers (1–5) quench the radical intermediates leading to MB degradation. EDTA-Na 2 mmol L^{-1} is shown to be the most active species precluding almost completely MB degradation due the scavenging of the TiO_2vbh^+ species. The relative importance of the species intervening in MB discoloration would be: vbh+ > $O_2^{\bullet-}/HO_2^\bullet$ > $1O_2$ > $OH^\bullet$. A simplified MB-degradation mechanism including the radical species leading to the dye degradation is suggested below:

$$MB + [PE\text{-}TiO_2] + light \rightarrow [PE\text{-}TiO_2*]MB \rightarrow MB^{+\cdot} + PE\text{-}TiO_2cbe\text{-} \quad (6)$$

$$PE\text{-}TiO_2cbe\text{-} + O_2 + H^+ \Leftrightarrow HO_2^\bullet E_0 - 0.05NHE[36] \quad (7)$$

$$PE\text{-}TiO_2cbe\text{-} + O_{2ads} \rightarrow {O_2^{\bullet-}}_{ads} E_0 - 0.16NHE \quad (8)$$

$$PE\text{-}TiO_2vbh^+ + {OH^-}_{ads} \rightarrow OH^\bullet E_0 - 1.90NHE \quad (9)$$

$$PE\text{-}TiO_2vbh^+ + {H_2O}_{ads} \rightarrow {OH^\bullet}_{ads} + H^+ \quad (10)$$

$$O_2^{\bullet-} + H+ \rightarrow HO_2^\bullet pK_a 4.8 \quad (11)$$

In Reaction (11) the $HO_2^\bullet$ radical is stable at pH <4.8, above this pH more than 50% is present in the form of $O_2^{-\bullet}$. The MB initial pH for solutions in evaluated in Fig. 5 was 6.1–6.2 and the final pH was 4.6–4.7 after 6 h irradiation. This is more than a tenfold increase in the solution H^+-concentration which would favor the back reaction and therefore the build up of the $HO_2^\bullet$ radical in Eq. (7). Eq. (10) is the most important reaction leading to MB degradation due to: a) the strong scavenging effect of the vbh+ previously shown in Fig. 5 by EDTA-Na 2 mmol L^{-1}, b) the observed increase in acidity of the MB solution far above one pH unit-unot and finally c) the $OH^\bullet$-radicals in Eq. (10) undergo the one electron reduction reaction $OH^\bullet/OH^-$ with E_0 1.90 NHE *vs* $HO_2^{\bullet-}$ radicals undergoing the reduction $O_2^{\bullet-}/HO_2^\bullet$ at a somewhat lower level of E_0 0.75 NHE.

3.4. Temporal evolution of radicals on PE-TiO_2, OH-radical detection by fluorescence and optical absorption by PE-TiO_2 samples

Fig. 6a shows that the MB discoloration within 3 h is almost complete at pH 3. Fig. 6b shows the results for the same solution as used in Fig. 6a but at pH 6. A faster MB discoloration rate was observed at pH 6. Next, we added benzoquinone (BQ) 2 mmol L^{-1} to the MB-solution at pH 3. The MB discoloration shown in Fig. 6c was slower compared to the discoloration without addition of BQ (Fig. 6a). BQ

is added next at pH 6. Fig. 6d shows faster discoloration kinetics compared to the data reported in Fig. 6c. This due to the effect of the non-protonated superoxide anion-radical ($O_2^{\bullet -}$) being more effective than the $HO_2^{\bullet}$ present at pH 3, based on what explained for Reaction (11). The diffusion controlled electron transfer at pH 6 is shown in Eq. (12).

$$BQ + O_2^{\bullet -} \rightarrow BQ^- + O_2 \quad (12)$$

Fig. 6e shows the effect of the addition of the $^1O_2$ quencher NaN_3 (20 mmol L^{-1}) at pH 3. A strong decrease is observed in the MB discoloration initial stages <1 h indicating that the oxygen singlet $^1O_2$ intervenes from the beginning in MB discoloration. An almost similar effect was observed for the NaN_3 addition to a MB solution at pH 6. The NaN_3 effect decreases strongly after 1 h (Fig. 6e). This suggests that NaN_3 the $^1O_2$ is produced in the initial reaction stages and subsequently reacts with long-lived intermediates produced during MB degradation further generating $O_2^{\bullet -}$ [31].

$$MB\text{long-lived intermediates} + {}^1O_2 \rightarrow \text{intermediate cations}(D^+) + O_2^{\bullet -} \quad (13)$$

Next BQ + NaN_3 were added at pH3 and pH6 to sort out the effects of the combined quenchers on MB-discoloration as a function of the solution pH. Fig. 6f) shows that at pH 3, the added scavengers were more effective than at pH 6 (Fig. 6g)). MB-discoloration seems to be controlled mainly by the $HO_2^{-\bullet}/O_2^{-\bullet}$ as suggested by the equilibrium in Eq. (11).

Fig. 7 shows the increase in $OH^{\bullet}$ species as a function of the PE-TiO_2 irradiation time. The increase in the fluorescence intensity is proportional to the concentration of $OH^{\bullet}$ in solution. Details of the analysis have been already described in the Section 2 [30]. This data further confirms the presence of $OH^{\bullet}$ radicals during MB-discoloration as previously shown in a qualitatively way in Fig. 5. The optical density (OD) of the different PE-TiO_2 films is shown in Fig. 8. TiO_2 absorption is below 400 nm and in Fig. 8a tail absorption is seen at longer wavelengths. For this reason a second set of measurements was carried out in an instrument designed to measure reflectance and transmittance of films (aRTie (F2-RT) Filmetrics) [27].

3.5. Implications of the hydrophobic-hydrophilic transformation under TiO_2 band-gap irradiation and dark reverse reaction of PE-TiO_2 films

Fig. 9a shows the reduction in the CA of the PE-TiO_2 film under mercury light irradiation from the hydrophobic CA of 92° at time zero to a value < 5° within ~5 h The hydrophobic-hydrophilic transformation is induced by the photo-generated holes of the TiO_2 involving trapped lattice oxygen sites [2,3,37]. The reverse transformation to the initially hydrophobic PE-TiO_2 was observed to be complete in about 100 h. This implies that the most favorable discoloration time for solutions of MB 1×10^{-5} M during the repetitive use of a PE-TiO_2 film, requires a long recovery of the photocatalyst.

Fig. 9b shows the hydrophobic to hydrophilic transformation as a function of Υ_S under mercury light irradiation within ~5 h and the back transformation to the hydrophobic initial state in the dark as a function of Υ_S within 100 h. This plot was obtained by integrating "cos θ" in the Young's equation. The wettability is commonly evaluated in terms of the contact angle (CA/θ) in Young's equation [2,3].

$$\Upsilon_S = \Upsilon_{SL} + \Upsilon_L \cdot \cos\theta \quad (14)$$

In Eq. (14) Υ_S and Υ_L are the surface free energies per unit area of the solid and liquid respectively, and Υ_{SL} is the interfacial free energy per unit area. In addition, Υ_{SL} can be approximated using the Girifalco-Good equation [30], with Υ_S and Υ_L, as

$$\Upsilon_{SL} = \Upsilon_S + \Upsilon_L - \Phi(\Upsilon_S \Upsilon_L)^{1/2} \quad (15)$$

Here, Φ is a constant parameter ranging from 0.6 to 1.1, depending on the solid. In addition, Υ_L is the water surface free energy, which has a constant value of 74 mJm-^{2}. Therefore, by combining Eq. (14) and (15), the Υ_S can be expressed as:

$$\Upsilon_S = C(1 + \cos\theta)^2 (C : \text{constant}) \quad (16)$$

Table 2
Surface percentage atomic concentration of PE-TiO_2 during MB discoloration as determined by XPS. The first row refers to a samples of PE-TiO_2 contacted with MB for a short period in the dark.

Reaction time (h)	C	N	O	S	Ti
0	57.0	0.43	30.7	0.20	11.65
0.5	57.6	2.10	29.1	0.30	10.80
1	59.6	1.92	27.3	0.84	10.25
2	68.3	2.57	20.8	0.62	7.58
4	68.0	2.74	21.6	0.77	6.86
8	55.0	1.48	31.4	0.52	11.50

3.6. X-Ray photoelectron spectroscopy (XPS) peak changes during the MB-discoloration process

Table 2 presents the atomic surface concentration percentage variation of several elements during the discoloration of MB on PE-TiO_2 photocatalyst. It is readily seen that the C, N and S content increase during the first 4 h due to the residues (intermediates long-lived organic decomposition products, sulfate-ions, nitrate-ions) accumulating on the film surface. After 8 h, their percentages decrease since the long-lived C-residues convert into CO_2 and the oxidation of N and S in the presence of air (O_2) takes place, being converted into volatile *N*- and *S*-species. The *O*-content and the Ti-content seem to decrease within the first 4 h, as the MB-decomposition residues shield the O and Ti-signal of the PE-TiO_2 surface. Once the organic and N, S fragments from MB degradation are removed after 8 h, the Ti initial surface content is re-established. This shows the catalytic removal of MB is possible by the PE-TiO_2 photocatalyst.

Fig. 10 shows the peaks of Ti, C, and O before and after 4 h irradiation of a solution MB 3×10^{-5}. The carbon C1s at 284.6 eV was used as the reference for the peak positions of Ti, C, and O the XPS spectrogram [38,39]. The Shirley correction was used to correct the electrostatic charging effect during the XPS measurement [40]. The Ti2p doublet peak binding energy BE is seen to shift from 457.01 eV to 457.26 eV. This suggests the MB-degradation proceeds concomitant with redox reactions in the PE-TiO_2 film. This is a further evidence for the photocatalysis proceeding through Ti^{3+}/Ti^{4+} species on the surface of the films since the peak shift is > 0.2 eV [38]. The shift in the C1s BE originating from the PE is seen by the peak shift from 283.38 eV to 283.12 eV. This again confirms redox reactions occurring in the C- within the time of MB discoloration. Redox behavior was again observed during the O1s peak shift in the last graph of Fig. 10.

4. Conclusions

A comprehensive, detailed and systematic study is presented for a stable PE-TiO_2 film leading to the degradation of MB with acceptable kinetics under TiO_2 band-gap irradiation. This study presents several findings by the PE-TiO_2 films related to important photocatlytic issues. An innovative adhesive coating of TiO_2 on PE is presented prepared in an environmentally friendly way, at low temperatures and not requiring expensive instrumenta-

tion. Evidence is presented for the PE-TiO_2 films able to degrade MB in a repetitive way showing the same MB-degradation kinetics. Scavenging experiments identifying the ROS species leading to MB degradation are reported for the first time. The TiO_2vbh+ was shown to be the most effective species leading to MB-degradation. The diffusion length for the $HO_2^{\bullet}$ and $OH^{\bullet}$ radicals was estimated reaching short distances away from the PE-TiO_2 films. The first evidence is presented for the PE-TiO_2 contact angle (CA) conversion from the initial hydrophobic (92°) to super-hydrophilic values (<5°). The time of the conversion was concomitant with the MB-discoloration time (5 h). The PE-TiO_2 films show a potential for practical applications to degrade dyes in water-treatment due to their stable repetitive photocatalytic performance.

Acknowledgments

We thank the EPFL and the EC7th Limpid FP project (Grant No. 3101177) for financial support and the COST Action MP1106 for interactive discussions during the course of this work. We thank S. Rtimi (EPFL) for the help with the experimental work during this study.

References

[1] A. Linsebigier, G. Lu, J. Yates, Chem. Rev. 95 (1995) 735–758.
[2] A. Fujishima, X. Zhang, D. Tryck, TiO_2 Surf. Sci. Rep. 63 (2008) 515–582.
[3] J. Schneider, M. Matsuoka, M. Takeuchi, J. Zhang, Y. Horiuchi, M. Anpo, D. Bahnemann, Chem. Rev. 114 (2014) 9919–9986.
[4] S. Banerjee, S. Pillai, P. Falaras, K. O'shea, J. Byrne, D. Dionysiou, J. Phys. Chem. 5 (2014) 2543–2554.
[5] A. Mills, S. Lee, J. Photochem. Photobiol. A 152 (2002) 233–247.
[6] C. Pulgarin, J. Kiwi, Chimia 50 (1996) 50–55.
[7] S. Ponce, E. Carpio, J. Venero, W. Estrada, J. Rodriguez, C. Reche, R. Candal, J. Adv. Oxid. Technol. 12 (2009) 81–86.
[8] S. Naskar, A. Pillai, M. Chanas, J. Photochem Photobiol. A 113 (1998) 257–264.
[9] Xu Zhao, Zongwei Li, Yi Chen, Liyi Shi, Yongfa Zhu, Appl. Surf. Sci. 254 (2008) 1825–1832.
[10] K. Tennakone, C. Tilakaratne, I. Kottegoda, J. Photochem, Photobiol. A 87 (1995) 177–179.
[11] B. Ohtani, S. Adzuma, H. Miyadzu, S.-I. Nishimoto, T. Kagiya, Polym. Degrad. Stab. 23 (1989) 271–278.
[12] S. Singh, H. Mahalingan, P.K. Singh, Appl. Catal. A. 462–463 (2013) 178–195.
[13] A. Mills, S. Le Hunte, J. Photochem, Photobiol. A 108 (1997) 1–35.
[14] A-M Braun, M-T Maurette, E. Oliveiros, Technologie Photochimique, chapter 12, 1986, Presses Polytechniques Romandes, Lausanne.
[15] A. Dutschke, C. Diegelman, P. Lobman, J. Mater. Chem. 13 (2003) 1058–1063.
[16] N. Tchoul, S. Fillery, H. Fillery, L. Drummy, M. Durstock, R. Vaia, Chem. Mater. 22 (2010) 1749–1759.
[17] C. Ye, H. Li, A. Ciao, Q. Gao, X. Zeng, J. Macromol. Sci. Part A 48 (2011) 309–314.
[18] A. Mesgane, M. Abdel, P. Simon, P. Jegou, G. Deniau, S. Palacin, J. Mater. Sci. 46 (2011) 6332–6338.
[19] S. Lu, S. Sun, J. Liu, L. Zeng, H. Liu, X. Zhaio, J. Mater. Sci. Mater. Electron. 23 (2012) 251–256.
[20] A. Essawy, A. Ali, M. Abdel-Mottaleb, J. Hazard. Mater. 157 (2008) 547–552.
[21] Yu Zhiyong, E. Mielczarski, J. Mielczarski, D. Laub, Ph Buffat, U. Klehm, P. Albers, K. Lee, A. Kulik, L. Kiwi-Minsker, A. Renken, J. Kiwi, Water Res. 41 (2007) 862–874.
[22] Yu Zhiyong, J. Mielczarski, E. Mielczarski, D. Laub, L. Minsker-Kiwi, J. Kiwi, J. Mol. Catal. A 260 (2006) 227–234.
[23] Yu. Zhiyong, D. Laub, M. Bensimon, J. Kiwi, Inorg. Chim. Acta 361 (2008) 589–594.
[24] S. Rtimi, C. Pulgarin, R. Sanjines, V. Nadtochenko, J.-C. Lavanchy, J. Kiwi, ACS Appl. Mater. Interfaces 7 (2015) 12832–12839.
[25] Sami Rtimi, Jelena Nesic Cesar Pulgarin, Rosendo Sanjines, Michael Bensimon and John Kiwi, Interface Focus, 2015, 5/rsfs. 2014.0046.
[26] Sami Rtimi, Rosendo Sanjines, Cesar Pulgarin, Andrej Kulik, John Kiwi, Surf. Coat. Technol. 254 (2014) 333–343.
[27] S. Rtimi, C. Pulgarin, R. Sanjines, J. Kiwi, Appl. Catal. B 162 (2015) 236–244.
[28] A. Mills, J. Wang, J. Photochem, Photobiol. A 127 (1999) 123–134.
[29] X. Qiu, M. Miyaguchi, K. Sunada, M. Minoshima, M. Liu, Y. Lu, D. Li, Y. Shimodaira, Y. Hosogi, Y. Kuroda, K. Hashimoto, ACS Nano 6 (2012) 1609–1618.
[30] K. Ishibashi, A. Fujishima, T. Watanabe, K. Hashimoto, Electrochem. Commun. 2 (2000) 207–210.
[31] A. Houas, H. Lachheb, M. Ksibi, E. Elaloui, C. Guillard, J.-M. Herrmann, Appl. Catal. B 31 (2001) 145–157.
[32] T. Egerton, C. King, J. Oil Color Chem. Assoc. 62 (1979) 386–391.
[33] P. Piccinini, C. Minero, M. Vincenti, E. Pelizzetti, J. Chem. Soc. Faraday 93 (1997) 1993–2000.
[34] K. Patal, L. Wilson, J. Chem. Soc. Faraday Trans. 69 (1972) 814–825, 1.
[35] K. Vignodopal, P. Kamat, J. Photochem. Photobiol. A 10 (1994) 1767–1772.
[36] P. Wardman, J. Phys. Chem. Ref. Data 18 (1989) 1637–1755.
[37] S. Rtimi, C. Pulgarin, R. Sanjines, J. Kiwi, RSC Adv. 3 (2013) 16345–16348.
[38] C.D. Wagner, E.L. Davis, G.E. Müllenberg, (Ed) Handbook of X-Ray Photoelectron Spectroscopy, Minnesota, 1979, USA.
[39] J. Nogier, M. Delamar, P. Ruiz, P. Albers, J. Kiwi, (1999) 109–123.
[40] D.A. Shirley, Phys. Rev. B5 (1972) 4709–4714.